Radboud Repository

Radboud University Nijmegen

PDF hosted at the Radboud Repository of the Radboud University Nijmegen

This full text is a publisher's version.

For additional information about this publication click this link.
http://hdl.handle.net/2066/16106

Please be advised that this information was generated on 2014-11-12 and may be subject to change.

Ab initio collision-induced polarizability, polarized and depolarized Raman spectra, and second dielectric virial coefficient of the helium diatom

Robert Moszynski
Institute of Theoretical Chemistry, Nijmegen–SON Research Center, University of Nijmegen, Toernooiveld, 6515 ED Nijmegen, The Netherlands
and Department of Chemistry, University of Warsaw, ul. Pasteura 1, 02-093 Warsaw, Poland

Tino G. A. Heijmen, Paul E. S. Wormer, and Ad van der Avoird
Institute of Theoretical Chemistry, Nijmegen–SON Research Center, University of Nijmegen, Toernooiveld, 6525 ED Nijmegen, The Netherlands

(Received 15 November 1995; accepted 23 January 1996)

Symmetry-adapted perturbation theory has been applied to compute the interaction-induced polarizability for the helium diatom. The computed polarizability invariants have been analytically fitted, and used in quantum-dynamical calculations of the binary collision-induced Raman spectra. The predicted intensities of the depolarized spectrum are in good agreement with the experimental data [M.H. Proffitt *et al.*, Can. J. Phys. **59**, 1459 (1981)]. The computed polarized spectrum shows agreement with the experiment within the large experimental uncertainties. The calculated trace polarizability was also checked by comparison of computed second dielectric virial coefficients with the experimental data. The *ab initio* dielectric virial coefficients, including first and second quantum corrections, agree well with the experimental data from indirect measurements. © *1996 American Institute of Physics.* [S0021-9606(96)03016-2]

I. INTRODUCTION

Interactions between colliding atoms in gases or fluids lead to distortions of their charge distributions, so that a collisional pair of atoms possesses a polarizability in excess of the sum of polarizabilities of the isolated atoms. This excess polarizability, referred to as the interaction-induced or collision-induced polarizability is defined as the incremental part of the diatom polarizability tensor due to interatomic interactions, i.e., as the difference between the diatom polarizability tensor and the sum of polarizabilities of the noninteracting atoms.

The interaction-induced pair polarizabilities are responsible for a wide range of dielectric, refractive, and optical properties of gases and fluids.[1,2] Levine and Birnbaum[3] predicted that all Raman spectra of gases should have a component due to collision-induced changes in the polarizabilities, and it was first demonstrated by McTague and Birnbaum[4] that free argon atoms in a collisional encounter undergo transitions between translational states when interacting with photons. At very low densities the light scattering leads to the well-known Rayleigh–Brillouin process. At higher densities nearly exponential Stokes and anti-Stokes wings appear, with intensities proportional to the square of the gas density.[4,5] These components of the Raman spectra of gases (referred to as translational Raman effect) are due to the collision-induced light scattering, i.e., to the interaction-induced fluctuations of the polarizabilities of atoms and molecules. In particular, in atomic fluids the anisotropy of the polarizability tensor will give rise to the *depolarized* Raman spectrum, while the small trace polarizability will lead to the *polarized* Raman spectrum. Since the early work on argon, the collision-induced light scattering has been experimentally studied in several optically isotropic systems (see Refs. 6–8 for reviews).

Besides giving rise to the collision-induced light scattering, the interaction-induced polarizability invariants also affect the dielectric and refractive properties of gases. The trace polarizability determines the second virial coefficient of the dielectric Clausius–Mosotti function, while the square of the anisotropy of the interaction-induced polarizability tensor is related to the Kerr constant of gases and to the pressure-dependent depolarization ratio. At present, the second dielectric virial coefficients and Kerr constants are available for various atomic and molecular systems (see Refs. 9 and 10 for reviews of the experimental data).

The collision-induced polarizability of the He diatom has been investigated using various experimental techniques. Several studies of the collision-induced light scattering in helium have been reported in the literature.[11–19] Most of these measurements were done at high densities,[11–14] so the reported Raman intensities were affected by three-body contributions, and pure pair spectra had to be separated out[14] by applying some simplified models. Only the polarized and depolarized Raman spectra for the ^{3}He and ^{4}He gases reported by Proffitt, Keto, and Frommhold[18,19] were shown to be free from three-body contributions, i.e., the recorded Raman intensities showed the correct quadratic dependence on the gas density. Also the refractivity and second dielectric virial coefficients at various temperatures,[20–30] as well as the depolarization ratio[31] of the He gas have been reported.

Because of the small number of electrons involved, the interaction-induced polarizability of He_2 has been object of many *ab initio* studies.[32–39] Most of these studies[33–37] were done at the Hartree–Fock level of theory, neglecting important inter- and intra-atomic correlation effects. To our knowledge, the only correlated results for the collision-induced po-

 0021-9606/96/104(18)/6997/11/$10.00 © 1996 American Institute of Physics

larizability of He_2 were reported by Dacre.[38,39] These calculations were done using the configuration interaction method restricted to single and double excitations (CISD) and medium-size *spd* basis sets. In addition, also the long-range coefficients have been computed[40–42] for this system at various levels of approximation.

The quantum-mechanical theory[43–45] of the collision-induced Raman spectra is now well established, and *a priori* calculations of the Raman intensities are feasible, once the pair interaction potential and the interaction-induced polarizability are available. Various *ab initio* polarizability data for He_2 have been used to compute the collision-induced Raman spectra of the He diatom for comparison with experiment[19,46] (see also Ref. 6 for a review of these results). In an extensive theoretical study Dacre and Frommhold[46] have checked the accuracy of the *ab initio* CISD trace and anisotropy polarizabilities of He_2 (Ref. 39) by exposing them to the test of computing the observed Raman intensities. While the depolarized spectra computed from Dacre's polarizability[39] showed good agreement with the experiment for both isotopes of helium, the theoretical polarized spectrum was much less intense than the spectrum derived from the experiment.[46]

The reasons for the less satisfactory agreement between the theoretical and experimental polarized Raman spectra may be both on the theoretical and on the experimental sides. The experimental polarized spectrum is obtained as the difference of two nearly equal signals excited with different beam polarizations,[18,19] and the accuracy of the polarized intensities deduced from the experiment may be poor. On the other hand, the theoretical values of the interaction-induced trace may suffer from approximate corrections for the size inconsistency of the CISD method, the basis set superposition error, or basis set incompleteness. Finally, the computed polarized spectra showed[46] a rather strong dependence on the interatomic potential. The potentials used in the calculations of Ref. 46 differ from the best empirical potentials available at present.[47,48] Thus, an attempt to refine the accuracy of the *ab initio* polarizability invariants of He_2 and to check these by computing the Raman spectra is now in order.

We have shown[49] that the interaction-induced properties of collisional complexes can be accurately computed using the many-body formulation[50–56] of the symmetry-adapted perturbation theory (SAPT)[57–60] (see Ref. 61 for a recent review of SAPT). In the present paper we report SAPT calculations of the interaction-induced polarizability for the He diatom, and dynamical calculations of the polarized and depolarized Raman intensities. We also check the *ab initio* collision-induced polarizability by computation of the second dielectric virial coefficient, and comparison with the available experimental data. The plan of this paper is as follows. In Sec. II the SAPT calculations are briefly described, and the analytical fits to the computed points are presented. The formalism used in dynamical calculations is outlined in Sec. III. The results of SAPT and dynamical calculations are presented and discussed in Sec. IV. In Sec. V we report *ab initio* calculations of the second dielectric virial coefficient for He_2. Finally, in Sec. VI we present conclusions.

II. OUTLINE OF SAPT CALCULATIONS

A. Method and definitions

The interaction-induced polarizability $\Delta\alpha_{ij}$ of a pair of atoms A and B is defined as the excess polarizability of the collisional pair AB due to intermolecular interactions, i.e.,

$$\Delta\alpha_{ij}=\alpha_{ij}^{AB}-(\alpha_0^A+\alpha_0^B)\,\delta_{ij}\,, \tag{1}$$

where α_{ij}^{AB} is a component of the dimer polarizability tensor, and α_0^A and α_0^B denote polarizabilities of the isolated atoms A and B, respectively. Equation (1) can be conveniently rewritten as,

$$\Delta\alpha_{ij}=-\left(\frac{\partial^2 E_{\rm int}}{\partial F_i\,\partial F_j}\right)_{F_i=F_j=0}, \tag{2}$$

where $E_{\rm int}$ is the interaction energy for the dimer AB in the presence of a static, uniform electric field $\boldsymbol{F}$. Eq. (2) shows that the interaction-induced polarizability can be obtained from standard finite field calculations, if the field-dependent interaction energy can be computed. In the present paper we have utilized this possibility, i.e., we first performed calculations of the interaction energy in the static electric field using the symmetry-adapted perturbation theory, and subsequently obtained the interaction-induced polarizability components from finite difference formulas. Below we shortly summarize the SAPT *ansatz* for the field-dependent interaction energy $E_{\rm int}$. The components of the interaction-induced polarizability tensor $\Delta\alpha_{ii}$ have been obtained from the equation:

$$\Delta\alpha_{ii}=-\frac{E_{\rm int}(F_i)+E_{\rm int}(-F_i)-2E_{\rm int}(0)}{F_i^2}+O(F_i^4), \tag{3}$$

where the index $i=z$ or x denotes the direction along the dimer axis, or perpendicular to this axis, respectively.

In the calculations of the interaction energy in the static electric field we follow the approach proposed and tested in our recent paper[49] (see also Refs. 62–67 for applications to the interaction energy calculations). The SAPT interaction energy is represented as a sum of components corresponding to the Hartree–Fock ($E_{\rm int}^{\rm HF}$) and correlated ($E_{\rm int}^{\rm corr}$) levels of the theory,

$$E_{\rm int}=E_{\rm int}^{\rm HF}+E_{\rm int}^{\rm corr}\,. \tag{4}$$

The Hartree–Fock interaction energy can be decomposed as[68–71]

$$E_{\rm int}^{\rm HF}=E_{\rm pol}^{(10)}+E_{\rm exch}^{(10)}+E_{\rm ind,resp}^{(20)}+E_{\rm exch-ind,resp}^{(20)}+\delta E_{\rm int}^{\rm HF}\,, \tag{5}$$

where $E_{\rm pol}^{(10)}$ and $E_{\rm exch}^{(10)}$ are the electrostatic and exchange contributions, respectively, with complete neglect of the intraatomic correlation effects,[72] $E_{\rm ind,resp}^{(20)}$ and $E_{\rm exch-ind,resp}^{(20)}$ are the Hartree–Fock induction and exchange-induction energies, respectively, accounting for the coupled-Hartree–Fock type response, i.e., for the perturbation-induced modification of the Hartree–Fock potential,[70,71] and $\delta E_{\rm int}^{\rm HF}$ collects higher-order induction and exchange contributions.

At the correlated level, the SAPT interaction energy is represented by

$$E_{\rm int}^{\rm corr}=\epsilon_{\rm pol}^{(1)}+\epsilon_{\rm exch}^{(1)}+\epsilon_{\rm ind}^{(2)}+E_{\rm disp}^{(2)}+E_{\rm exch-disp}^{(2)}, \tag{6}$$

where $E_{\rm disp}^{(2)}$ is the dispersion energy, and $\epsilon_{\rm pol}^{(1)}$, $\epsilon_{\rm exch}^{(1)}$, and $\epsilon_{\rm ind}^{(2)}$ are the electron correlation contributions to the exact electrostatic ($E_{\rm pol}^{(1)}$), exchange ($E_{\rm exch}^{(1)}$), and induction ($E_{\rm ind}^{(2)}$) energies, respectively, i.e., $\epsilon_{\rm pol}^{(1)}\equiv E_{\rm pol}^{(1)}-E_{\rm pol}^{(10)}$, $\epsilon_{\rm exch}^{(1)}\equiv E_{\rm exch}^{(1)}-E_{\rm exch}^{(10)}$, and $\epsilon_{\rm ind}^{(2)}\equiv E_{\rm ind}^{(2)}-E_{\rm ind,resp}^{(20)}$. Each term on the r.h.s. of Eq. (6) can be evaluated using many-body perturbation expansions with respect to the intra-atomic electronic correlation,

$$E_{\rm pol}^{(k)}=\sum_{n=0}^{\infty}E_{\rm pol}^{(kn)} \quad \text{and} \quad E_{\rm exch}^{(k)}=\sum_{n=0}^{\infty}E_{\rm exch}^{(kn)}, \tag{7}$$

where $E_{\rm pol}^{(kn)}$ and $E_{\rm exch}^{(kn)}$ are the polarization and exchange corrections of kth order in the intermolecular interaction and nth order in the intra-atomic correlation. In the present study the contributions to $E_{\rm int}^{\rm corr}$ were approximated as follows:

$$\epsilon_{\rm pol}^{(1)}=E_{\rm pol,resp}^{(12)}+E_{\rm pol,resp}^{(13)}, \tag{8}$$

$$\epsilon_{\rm exch}^{(1)}=E_{\rm exch}^{(11)}+E_{\rm exch}^{(12)}+\Delta_{\rm exch}^{(1)}({\rm CCSD}), \tag{9}$$

$$\epsilon_{\rm ind}^{(2)}=\epsilon_{\rm ind}^{(22)}, \tag{10}$$

$$E_{\rm disp}^{(2)}=E_{\rm disp}^{(20)}+E_{\rm disp}^{(21)}+E_{\rm disp}^{(22)}, \tag{11}$$

$$E_{\rm exch-disp}^{(2)}=E_{\rm exch-disp}^{(20)}. \tag{12}$$

The electrostatic corrections $E_{\rm pol,resp}^{(1n)}$ are defined as in Ref. 53. The first-order exchange components $E_{\rm exch}^{(1n)}$ are defined as in Refs. 54 and 55, while $\Delta_{\rm exch}^{(1)}$(CCSD) is the sum of higher-order terms (in the intra-atomic correlation) obtained by replacing the first and second-order cluster operators entering the expression for $E_{\rm exch}^{(12)}$ by the converged coupled-cluster singles and doubles (CCSD) operators.[54] The dispersion components $E_{\rm disp}^{(2n)}$ are derived in Ref. 52. The induction-correlation term $\epsilon_{\rm ind}^{(22)}$ represents the true correlation contribution to the nonrelaxed $E_{\rm ind}^{(22)}$ correction, as defined in Ref. 56. Finally, $E_{\rm exch-disp}^{(20)}$ is the so-called "Hartree–Fock" exchange-dispersion energy.[73]

The SAPT approach applied in the present paper is expected to give more accurate results for the interaction-induced polarizability tensor of He_2 than the CISD model used by Dacre.[38,39] Unlike the CISD method, the perturbation theory approach is size consistent, and all contributions to the collision-induced trace and anisotropy vanish in the limit $R\rightarrow\infty$. Although Dacre's calculations[39] included approximate corrections for the size-consistency error, it is not *a priori* obvious that the resulting polarizability components are correct. In SAPT calculations the components of the interaction-induced polarizability tensor are obtained directly (not as a difference of large numbers), so they are free from basis set superposition errors plaguing correlated supermolecule calculations. Let us also mention that our approach accounts for the major part of the triple-excitation contribution to the dispersion term, while the CI method restricted to single and double excitations does not.

B. Computational details

Calculations of the interaction-induced polarizability for the He dimer have been performed for ten interatomic distances R ranging from $R=3$ bohr to $R=10$ bohr. For the helium atom we used a $[5s4p3d2f]$ basis. The s orbitals were represented by the (61111) contraction of Van Duijneveldt's $10s$ set,[74] and the exponents of the polarization functions were taken from Ref. 75. To check the basis set convergence, for $R=3$, 4, and 5 bohr we performed additional calculations in two $spdfg$ basis sets: $[5s4p3d2f1g]$ and $[7s5p4d3f1g]$, and in a smaller $[5s3p2d]$ basis. The exponents of the polarization functions were again taken from Ref. 75. The spherical form of the polarization functions has been used (5 d functions and 7 f functions). In order to fully account for the charge-overlap effects all calculations have been done using the full dimer basis set.

The calculations have been performed with the SAPT system of codes.[76] In addition, full configuration interaction (FCI) results have been obtained from the program by Zarrabian *et al.*[77] The components of the interaction-induced polarizability tensor have been obtained by numerical differentiation of the field-dependent interaction energies, cf. Eq. (3). For both directions of the external electric field, its strength was equal to ± 0.001 a.u.. In addition, long-range van der Waals coefficients corresponding to the multipole-expanded electrostatic, induction, and dispersion polarizabilities[49] have been computed at the same level of theory and the same basis sets using the Polcor package.[78,79] These coefficients have been subsequently used in the analytical fits of the interaction-induced polarizabilities. We used the Boys–Bernardi counterpoise correction to eliminate the basis set superposition error from the supermolecular Hartree–Fock calculations.[80]

As discussed in Ref. 46 the intensities of the collision-induced Raman spectra depend on the invariants of the interaction-induced polarizability tensor at the laser wavelength λ. Our SAPT calculations were done for $\lambda=\infty$, i.e., for the static case, and an extension of the SAPT theory to include the λ dependence would be very difficult. To investigate the importance of the wavelength dependence we have performed additional calculations using the supermolecule random phase approximation (RPA) and the second-order Møller–Plesset (MP2) approaches.[78,79]

C. Analytical fits

The intensities of the collision-induced Raman transitions and the second dielectric virial coefficients depend on the invariants of the interaction-induced polarizability tensor. Therefore in what follows we will consider the anisotropy β and the trace α, defined through the components of the tensor by the equations:

$$\beta=\Delta\alpha_{zz}-\Delta\alpha_{xx}, \tag{13}$$

$$\alpha=\frac{1}{3}(\Delta\alpha_{zz}+2\Delta\alpha_{xx}). \tag{14}$$

In SAPT calculations different physical contributions to the polarizability invariants exhibit different distance dependence, and each contribution to the trace and anisotropy of the interaction-induced polarizability can be fitted separately. Therefore, it is convenient to represent α and β as

$$\alpha=\alpha_{\rm pol}^{(1)}+\alpha_{\rm ind}^{(2)}+\alpha_{\rm disp}^{(2)}+\alpha_{\rm exch},$$
$$\beta=\beta_{\rm pol}^{(1)}+\beta_{\rm ind}^{(2)}+\beta_{\rm disp}^{(2)}+\beta_{\rm exch}. \tag{15}$$

Here $\alpha_{\rm pol}^{(1)}$ is the contribution to the trace due to electrostatic interactions (i.e., is obtained by differentiation of the field-dependent electrostatic energy $E_{\rm pol}^{(1)}=E_{\rm pol}^{(10)}+\epsilon_{\rm pol}^{(1)}$), $\alpha_{\rm ind}^{(2)}$ and $\alpha_{\rm disp}^{(2)}$ are contributions due to second-order induction and dispersion interactions, respectively, and $\alpha_{\rm exch}$ is obtained by differentiation of the total exchange energy, $E_{\rm exch}=E_{\rm exch}^{(10)}+\epsilon_{\rm exch}^{(1)}+E_{\rm exch-ind,resp}^{(20)}+E_{\rm exch-disp}^{(20)}+\delta E_{\rm int}^{\rm HF}$. Similar definitions hold for the contributions to β. One may note that each term on the r.h.s. of Eq. (15) has a well defined R dependence which is to a large extent determined by its multipole expansion (cf. Sec. III of our paper[49]). Therefore, we performed separate fits of the exchange, electrostatic, induction, and dispersion contributions to α and β.

It is well known that the exchange terms $\alpha_{\rm exch}$ and $\beta_{\rm exch}$ depend exponentially on R, so we represented the exchange components by the functions,

$$\alpha_{\rm exch}(R)=(A_{\rm exch}^{(\alpha)}+B_{\rm exch}^{(\alpha)}R)\exp(-a_{\rm exch}^{(\alpha)}R)+(C_{\rm exch}^{(\alpha)}+D_{\rm exch}^{(\alpha)}R)\exp(-b_{\rm exch}^{(\alpha)}R), \tag{16}$$

$$\beta_{\rm exch}(R)=(A_{\rm exch}^{(\beta)}+B_{\rm exch}^{(\beta)}R)\exp(-a_{\rm exch}^{(\beta)}R)+(C_{\rm exch}^{(\beta)}+D_{\rm exch}^{(\beta)}R)\exp(-b_{\rm exch}^{(\beta)}R), \tag{17}$$

where the parameters $A_{\rm exch}^{(\alpha)}$, $B_{\rm exch}^{(\alpha)}$, $a_{\rm exch}^{(\alpha)}$, $C_{\rm exch}^{(\alpha)}$, $D_{\rm exch}^{(\alpha)}$, and $b_{\rm exch}^{(\alpha)}$, and similar parameters for $\beta_{\rm exch}$ were determined using the weighted least-square method with weights exponential in R.

The electrostatic contribution to β was represented by the damped multipole term and an exponential function representing the short-range penetration terms due to the charge overlap,

$$\beta_{\rm pol}^{(1)}(R)=(A_{\rm pol}^{(\beta)}+B_{\rm pol}^{(\beta)}R)\exp(-a_{\rm pol}^{(\beta)}R)+\frac{C_{3,\rm pol}^{(\beta)}}{R^3}f_3(R;b_{\rm pol}^{(\beta)}), \tag{18}$$

where $f_n(R;b)$ is the damping function in the Tang–Toennies form,[81]

$$f_n(R;b)=1-\exp(-bR)\sum_{k=0}^{n}\frac{(bR)^k}{k!}, \tag{19}$$

and the parameters $A_{\rm pol}^{(\beta)}$, $B_{\rm pol}^{(\beta)}$, $a_{\rm pol}^{(\beta)}$, and $b_{\rm pol}^{(\beta)}$ were determined using the weighted least-square method with R^3 weights. One may note that the long-range coefficient $C_{3,\rm pol}^{(\beta)}$ was *not* fitted but computed *ab initio* in the same basis set and at the same level of theory as $\beta_{\rm pol}^{(1)}$.

In the multipole approximation the electrostatic contribution to the interaction-induced polarizability tensor of two S-state atoms is traceless.[49] Thus, $\alpha_{\rm pol}^{(1)}$ is exclusively due to short-range charge-overlap effects. Therefore, we represented $\alpha_{\rm pol}^{(1)}$ by the function,

$$\alpha_{\rm pol}^{(1)}(R)=(A_{\rm pol}^{(\alpha)}+B_{\rm pol}^{(\alpha)}R)\exp(-a_{\rm pol}^{(\alpha)}R), \tag{20}$$

where the parameters $A_{\rm pol}^{(\alpha)}$, $B_{\rm pol}^{(\alpha)}$, and $a_{\rm pol}^{(\alpha)}$ were determined using the weighted least-square method with weights exponential in R.

The induction components $\beta_{\rm ind}^{(2)}$ and $\alpha_{\rm ind}^{(2)}$ were represented as sums of damped multipole expansions and exponential functions representing the short-range charge-overlap contributions

$$\alpha_{\rm ind}^{(2)}(R)=(A_{\rm ind}^{(\alpha)}+B_{\rm ind}^{(\alpha)}R)\exp(-a_{\rm ind}^{(\alpha)}R)+\sum_{n=6}^{10}{}'\,f_n(R;b_{\rm ind}^{(\alpha)})C_{n,\rm ind}^{(\alpha)}R^{-n}, \tag{21}$$

$$\beta_{\rm ind}^{(2)}(R)=(A_{\rm ind}^{(\beta)}+B_{\rm ind}^{(\beta)}R)\exp(-a_{\rm ind}^{(\beta)}R)+\sum_{n=6}^{10}{}'\,f_n(R;b_{\rm ind}^{(\beta)})C_{n,\rm ind}^{(\beta)}R^{-n}, \tag{22}$$

where the prime on the summation symbol reminds us that the summation is restricted to even terms. The induction long-range coefficients $C_{n,\rm ind}^{(\alpha)}$ and $C_{n,\rm ind}^{(\beta)}$ are defined as in Sec. III of Ref. 49. These coefficients were *not* fitted but computed *ab initio* in the same basis set and at the level of theory corresponding to the fitted functions $\alpha_{\rm ind}^{(2)}(R)$ and $\beta_{\rm ind}^{(2)}(R)$. We assumed the damping function $f_n(R;b)$ in the Tang–Toennies form,[81] cf. Eq. (19). The parameters $A_{\rm ind}^{(\alpha)}$, $B_{\rm ind}^{(\alpha)}$, $a_{\rm ind}^{(\alpha)}$, and $b_{\rm ind}^{(\alpha)}$, and similar parameters for $\beta_{\rm ind}^{(2)}$, were determined using the weighted least-square method with R^6 weights.

The analytical representations of the dispersion contributions were the same as those of the induction terms, Eqs. (21) and (22), with the induction long-range coefficients $C_{n,\rm ind}^{(\alpha)}$ and $C_{n,\rm ind}^{(\beta)}$ replaced by the dispersion long-range coefficients $C_{n,\rm disp}^{(\alpha)}$ and $C_{n,\rm disp}^{(\beta)}$, defined as in Sec. III of Ref. 49. Again, these coefficients were *not* fitted but computed *ab initio* in the same basis set and at the level of theory corresponding to the fitted functions $\alpha_{\rm disp}^{(2)}(R)$ and $\beta_{\rm disp}^{(2)}(R)$. Here too, the damping function was assumed in the Tang–Toennies form.

The comparison of the final fitted functions with the *ab initio* points on which the fits were based shows that the typical approximation error is of the order of 0.4%. The only exception is, for obvious reasons, the region where the trace goes through zero. The values of the parameters are reported in Tables I and II. Fortran subroutines for generating the trace and anisotropy are available from the authors at the electronic mail address avda@theochem.kun.nl.

III. OUTLINE OF DYNAMICAL CALCULATIONS

The theory of collision-induced Raman spectra is well understood.[43,44] Below we only give a short summary. The laser light of wave number ω_0 is scattered inelastically by the interacting atoms. The intensities of the depolarized and polarized scattered light are given by

TABLE I. Parameters defining analytical fits to the computed electrostatic and exchange components of the collision-induced trace and anisotropy of the He_2 polarizability. All parameters are in proper powers of hartree and bohr.

		$\alpha(R)$		$\beta(R)$
Exchange	$A^{(\alpha)}_{exch}$	121.100	$A^{(\beta)}_{exch}$	−2580.967
	$B^{(\alpha)}_{exch}$	−80.663	$B^{(\beta)}_{exch}$	−442.347
	$a^{(\alpha)}_{exch}$	1.870	$a^{(\beta)}_{exch}$	1.655
	$C^{(\alpha)}_{exch}$	9.111	$C^{(\beta)}_{exch}$	2763.529
	$D^{(\alpha)}_{exch}$	−0.989	$D^{(\beta)}_{exch}$	−146.728
	$b^{(\alpha)}_{exch}$	1.160	$b^{(\beta)}_{exch}$	1.487
Electrostatics	$A^{(\alpha)}_{pol}$	−74.003	$A^{(\beta)}_{pol}$	−96.632
	$B^{(\alpha)}_{pol}$	32.771	$B^{(\beta)}_{pol}$	47.124
	$a^{(\alpha)}_{pol}$	2.153	$a^{(\beta)}_{pol}$	2.055
			$b^{(\beta)}_{pol}$	2.054
			$C^{(\beta)}_{3,pol}$	11.377

$$D(\nu)=\tfrac{2}{15}\omega^3\omega_0 G(\nu), \tag{23}$$

$$P(\nu)=\omega^3\omega_0 A(\nu), \tag{24}$$

where ν is the frequency shift, $\omega=\omega_0-2\pi\nu/c$, and c is the speed of light. The frequency shift ν is negative for the Stokes and positive for the anti-Stokes lines. The spectral functions of the anisotropy and trace, $G(\nu)$ and $A(\nu)$, can be written as,

$$G(\nu)=\frac{2hc\lambda_B^3}{(2I+1)^2}\sum_{J,J'} g_J(2J+1) \times\int_0^\infty dE\; e^{-E/k_BT} b^J_{J'}|\langle E',J'|\beta(R)|E,J\rangle|^2, \tag{25}$$

$$A(\nu)=\frac{2hc\lambda_B^3}{(2I+1)^2}\sum_{J} g_J(2J+1) \times\int_0^\infty dE\; e^{-E/k_BT}|\langle E',J|\alpha(R)|E,J\rangle|^2, \tag{26}$$

TABLE II. Parameters defining analytical fits to the computed induction and dispersion components of the collision-induced trace and anisotropy of the He_2 polarizability. All parameters are in proper power of hartree and bohr.

		$\alpha(R)$		$\beta(R)$
Induction	$A^{(\alpha)}_{ind}$	−43.442	$A^{(\beta)}_{ind}$	−207.978
	$B^{(\alpha)}_{ind}$	29.966	$B^{(\beta)}_{ind}$	116.800
	$a^{(\alpha)}_{ind}$	2.266	$a^{(\beta)}_{ind}$	2.337
	$b^{(\alpha)}_{ind}$	1.782	$b^{(\beta)}_{ind}$	1.570
	$C^{(\alpha)}_{6,ind}$	9.653	$C^{(\beta)}_{6,ind}$	14.345
	$C^{(\alpha)}_{8,ind}$	42.118	$C^{(\beta)}_{8,ind}$	50.541
	$C^{(\alpha)}_{10,ind}$	334.021	$C^{(\beta)}_{10,ind}$	357.880
Dispersion	$A^{(\alpha)}_{disp}$	−2.360	$A^{(\beta)}_{disp}$	−6.145
	$B^{(\alpha)}_{disp}$	1.836	$B^{(\beta)}_{disp}$	3.329
	$a^{(\alpha)}_{disp}$	1.604	$a^{(\beta)}_{disp}$	1.649
	$b^{(\alpha)}_{disp}$	1.246	$b^{(\beta)}_{disp}$	1.709
	$C^{(\alpha)}_{6,disp}$	23.205	$C^{(\beta)}_{6,disp}$	13.504
	$C^{(\alpha)}_{8,disp}$	356.165	$C^{(\beta)}_{8,disp}$	646.947
	$C^{(\alpha)}_{10,disp}$	966.497	$C^{(\beta)}_{10,disp}$	−6213.695

where $E'-E=h\nu$, $J'=J,J\pm2$, h is the Planck constant, k_B is the Boltzmann constant, T denotes the temperature, $\lambda_B=(h^2/2\pi\mu k_BT)^{1/2}$ is the de Broglie wavelength, μ is the reduced mass of the collisional complex, and I and g_J designate the nuclear spin and nuclear spin statistical weight, respectively. The constants $b^J_{J'}$ are given by[82,83]

$$b^J_{J'}=(2J'+1)\begin{pmatrix} J' & J & 2\\ 0 & 0 & 0\end{pmatrix}^2, \tag{27}$$

where the expression in round brackets is a $3j$ symbol.[84] Finally, the matrix elements of the trace and anisotropy appearing in Eqs. (25) and (26) are defined as,

$$\langle E',J'|X(R)|E,J\rangle = \int_0^\infty \psi^*(R;E',J')X(R)\psi(R;E,J)dR, \quad X=\alpha \text{ or } \beta, \tag{28}$$

where the radial wave functions $\psi(R;E,J)$ are solutions of the radial Schrödinger equation describing the relative motion of the atoms in the potential $V(R)$,

$$-\frac{\hbar^2}{2\mu}\frac{d^2\psi}{dR^2}+\left[V(R)+\frac{\hbar^2J(J+1)}{2\mu R^2}-E\right]\psi=0, \tag{29}$$

subject to the energy normalization condition,

$$\int_0^\infty \psi^*(R;E,J)\psi(R;E',J)dR=\delta(E-E'). \tag{30}$$

Note that in Eqs. (25) and (26) we neglected transitions from a bound state to a continuum state, and vice versa. Numerical results reported in Refs. 44 and 6 show that even for heavier rare gas pairs these transitions contribute usually less than 2% of the total intensity at any frequency shift. Since the He dimer is bound by 1.684 mK (Ref. 47) only, the contribution from bound-to-free and free-to-bound transitions at $T=296$ K should be even smaller. One may also note that the invariants of the interaction-induced polarizability tensor appearing in Eqs. (25) and (26) should be taken at the laser wave number ω_0. We have checked (cf. Sec. IV A for the discussion of this point) that the dependence of $\alpha(R)$ and $\beta(R)$ on ω_0 is very weak. Consequently, in the computations of the Raman spectra we used the static polarizability invariants from SAPT calculations.

The polarized and depolarized Raman intensities on the Stokes side were generated for the frequency shifts ranging from $\nu_{min}=-400$ cm^{-1} to $\nu_{max}=-10$ cm^{-1} with a step of 10 cm^{-1}. The Schrödinger equation (29) was solved using the Numerov method. The calculations were done with the BCONT program of Le Roy[85,86] adapted for the present purposes. The integration parameters, and the number of partial wave components were chosen to yield spectral functions of the anisotropy and trace converged to 3% at worst. In all calculations we have used the empirical He–He potential of Aziz *et al.*[47] The mass of ^{4}He was fixed at 4.002 60 a.m.u.[87]

TABLE III. Comparison of the interaction-induced trace and anisotropy of He_2 computed by SAPT with the FCI results (in 10^{-3} a.u.). All results were computed in the $[5s3p2d]$ basis.

	$R=3$ bohr		$R=4$ bohr		$R=5$ bohr		$R=8$ bohr
	$\alpha(R)$	$\beta(R)$	$\alpha(R)$	$\beta(R)$	$\alpha(R)$	$\beta(R)$	$\beta(R)$
SAPT	−130.034	175.693	−34.037	110.519	−5.439	78.365	22.368
FCI	−133.327	171.826	−34.262	111.912	−5.343	79.766	22.738
Δ[a]	−2.47%	2.25%	−0.66%	−1.24%	−1.80%	−1.76%	1.63%

[a]Relative error of the SAPT result with respect to the FCI result.

IV. NUMERICAL RESULTS

A. Interaction-induced polarizability of the He dimer

The residual error in the computed collision-induced polarizabilities is due to two sources: the neglect of higher-order terms in the SAPT expansion, and deficiencies of the basis set used in the calculations. Table III compares the interaction-induced trace and anisotropy computed at the full CI level with the SAPT results in the same basis set. For each of the distances considered in this table, SAPT reproduces the full CI results to within 3%. The only exception is the trace for $R \geqslant 6$ bohr but in this region of R the trace is very small and does not contribute to the polarized Raman intensities.[19] Although these calculations were done in the small spd basis, we expect the error to be largely independent of the basis set. It is reasonable then to assume that the effect of the truncation of the perturbation series on the computed interaction-induced polarizability invariants is smaller than 3%. It is worth noting that a similar estimate of the convergence rate of the SAPT expansion for the interaction potential of He_2 has been recently reported.[88]

The remaining errors are due to the basis set unsaturation. An examination of the basis set convergence presented in Table IV shows that the results in the $spdf$ basis are probably converged to within 2% or better. The extension of the basis set from the spd to $spdf$ quality improved the results by 1% on the average (the only exception is the trace for $R=5$ bohr, which changed by 7%). The next increase of the basis, i.e., the addition of a basis function of g symmetry, led only to changes smaller than 0.1% (again an exception is the trace for $R=5$ bohr, here the change amounts to 0.7%). Finally, an extension of the $spdfg$ basis with additional basis functions of s, p, d, and f symmetry changes the results by less than 2%. Certainly some of the errors discussed above will mutually cancel, so it is safe to assume that our results for the interaction-induced trace and anisotropy have an error of at most 5%.

In Table V we summarize the results of SAPT calculations, while in Figs. 1 and 2 we illustrate the behavior of the trace and anisotropy with the interatomic separation. For all distances the interaction-induced anisotropy is positive, and it decays slowly with R. The trace is much smaller because of the large cancellations involved. At short and intermediate distances the trace is negative. The sign change occurs at larger distances, where the trace itself is negligibly small. It is interesting to note that both the anisotropy and the trace result from a balance of the positive and negative contributions. For example, for $R \leqslant 5$ bohr $\alpha(R)$ represents about 50% of the negative exchange contribution $\alpha_{\mathrm{exch}}(R)$, and is approximately equal to the sum of the positive components, $\alpha^{(1)}_{\mathrm{pol}}(R)+\alpha^{(2)}_{\mathrm{ind}}(R)+\alpha^{(2)}_{\mathrm{disp}}(R)$. See also Ref. 49 for a more detailed discussion of this point. Also presented in Figs. 1 and 2 are the interaction-induced trace and anisotropy, as computed by Dacre[39] at the CISD level (including the size-consistency correction). In general the agreement between the two calculations is good. The largest difference in the anisotropy amounts to 2% at $R=3$ bohr, while the same number for the trace is 7% at $R=5$ bohr. The only exception is the trace at distances larger than $R=5$ bohr. Since in this region of R the trace is very small this disagreement is probably due to some numerical inaccuracies of the CISD calculations.

As discussed in Sec. III, the invariants of the interaction-induced polarizability tensor that enter the expression for the Raman intensities should be taken at the laser wavelength λ (corresponding to the wave number ω_0). Our the SAPT

TABLE IV. Basis set dependence of the interaction-induced trace and anisotropy of He_2. All results are in 10^{-3} a.u.

	$R=3$ bohr		$R=4$ bohr		$R=5$ bohr	
	$\alpha(R)$	$\beta(R)$	$\alpha(R)$	$\beta(R)$	$\alpha(R)$	$\beta(R)$
$[5s3p2d]$	−130.034	175.696	−34.037	110.519	−5.439	78.365
$[5s4p3d2f]$	−128.438	178.350	−32.984	111.930	−5.096	78.791
$[5s4p3d2f1g]$	−128.564	178.321	−32.971	111.864	−5.063	78.742
$[7s5p4d3f1g]$	−125.975	180.934	−32.393	112.856	−4.938	78.810

TABLE V. Interaction-induced trace and anisotropy of He_2 (in 10^{-3} a.u.) as function of the interatomic distance R (in bohr).

R	$\alpha(R)$	$\beta(R)$
3.0	−128.438	178.350
3.5	−69.903	132.262
4.0	−32.984	111.930
4.5	−13.801	95.118
5.0	−5.096	78.791
5.6	−1.131	61.138
6.0	−0.220	51.287
7.0	0.189	33.296
8.0	0.166	22.366
10.0	0.022	11.416

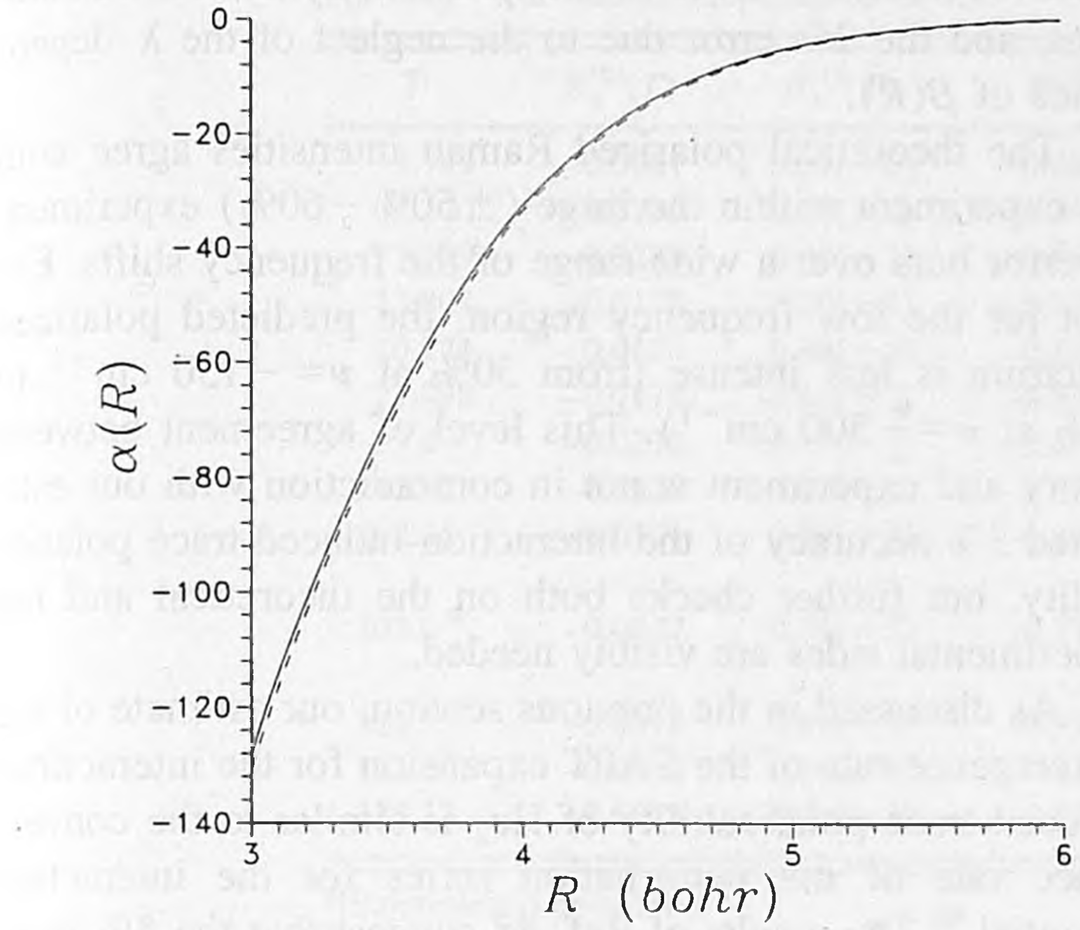

FIG. 1. Trace polarizability $\alpha(R)$ of He_2 (in 10^{-3} a.u.) as function of the interatomic separation R (in bohr). Full line represents the SAPT trace polarizability, while the dashed line shows the *ab initio* CISD results of Dacre (Ref. 39) corrected for the size-consistency error.

calculations were done at $\lambda=\infty$, and it is not *a priori* obvious whether $\alpha(R)$ and $\beta(R)$ at the laser wavelength $\lambda=5145$ Å would not change considerably. To investigate this point we have checked the importance of the λ dependence of $\alpha(R)$ and $\beta(R)$ using the supermolecule RPA and MP2 approaches. Although the RPA and MP2 levels of the theory are not expected to give very accurate results, the comparison of the polarizability invariants at $\lambda=\infty$ and $\lambda=5145$ Å will give an estimate of the λ dependence. The results of these additional calculations are reported in Table VI. As expected, the differences between the static and dynamic trace and anisotropy polarizabilities are small, and do not strongly depend on the interatomic distance. Hence, approximating $\beta(R)$ and $\alpha(R)$ in Eqs. (25) and (26) by their static values appears to be justified.

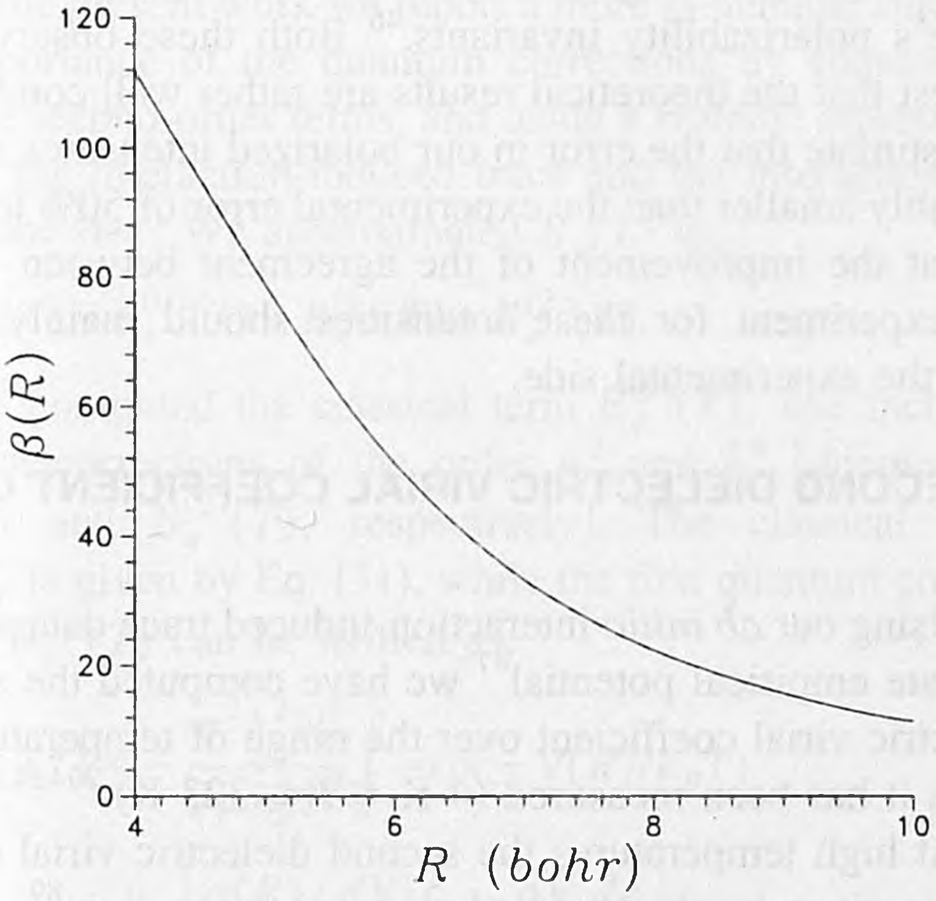

FIG. 2. Anisotropy $\beta(R)$ of He_2 (in 10^{-3} a.u.) as function of the interatomic separation R (in bohr). Full line represents the SAPT anisotropy, while the dashed line shows the *ab initio* CISD results of Dacre (Ref. 39) corrected for the size-consistency error.

TABLE VI. Wavelength dependence of the interaction-induced trace and anisotropy of He_2 (in 10^{-3} a.u.) computed using the supermolecule RPA and MP2 methods for selected interatomic distances R (in bohr).

R	λ	$\alpha^{RPA}(\lambda;R)$	$\beta^{RPA}(\lambda;R)$	$\alpha^{MP2}(\lambda;R)$	$\beta^{MP2}(\lambda;R)$
3.0	∞	−129.3	154.1	−128.0	156.8
	5145 Å	−131.7	155.8	−130.3	158.5
4.0	∞	−34.6	98.3	−33.4	99.8
	5145 Å	−35.4	99.2	−34.2	100.7
5.0	∞	−6.5	70.4	−5.8	71.2
	5145 Å	−6.7	71.3	−6.0	72.1

B. Collision-induced Raman spectrum of the helium diatom

In Table VII we summarize the results of quantum-dynamical calculations of the binary Raman spectra for the He diatom (see also Figs. 3 and 4 for graphical illustrations). An inspection of Table VII and Fig. 3 shows that the agreement of the theoretical depolarized Raman intensities with the results of measurements[19] is satisfactory. Most of the intensities agree within 3% or better. Only at very low and

TABLE VII. Comparison of the computed and measured depolarized and polarized Raman intensities (in 10^{-58} cm^6) of $^4He_2$ as function of the frequency shift (in cm^{-1}) at 296 K.

	$D(\nu)$		$P(\nu)$	
ν	Observed, Ref. 19	Computed	Observed, Ref. 19	Computed[a]
−30	37.0	42.6	1.94	1.29(1.43)
−50	25.7	29.3	1.32	1.30(1.44)
−70	17.5	18.7		1.28(1.41)
−90	11.8	12.2		1.22(1.35)
−100	9.62	9.90	1.18	1.19(1.31)
−110	7.84	8.05	1.27	1.15(1.27)
−120	6.40	6.56	1.34	1.11(1.23)
−130	5.25	5.36	1.37	1.07(1.18)
−140	4.31	4.39	1.41	1.03(1.13)
−150	3.56	3.60	1.42	0.99(1.08)
−160	2.93	2.96	1.45	0.94(1.03)
−170	2.42	2.44	1.48	0.90(0.98)
−180	1.99	2.01	1.53	0.85(0.94)
−190	1.68	1.66	1.52	0.81(0.89)
−200	1.42	1.38	1.52	0.77(0.84)
−210	1.22	1.14	1.51	0.73(0.79)
−220	1.05	0.948	1.50	0.68(0.75)
−230	0.899	0.789	1.48	0.65(0.71)
−240	0.762	0.657	1.44	0.61(0.67)
−250	0.649	0.549	1.38	0.57(0.63)
−260	0.548	0.459	1.32	0.54(0.59)
−270	0.464	0.384	1.24	0.50(0.55)
−280	0.385	0.322	1.15	0.47(0.52)
−290	0.318	0.270	1.07	0.44(0.49)
−300	0.259	0.227	0.99	0.42(0.45)

[a]In parentheses, polarized Raman intensities computed from the scaled polarizability trace.

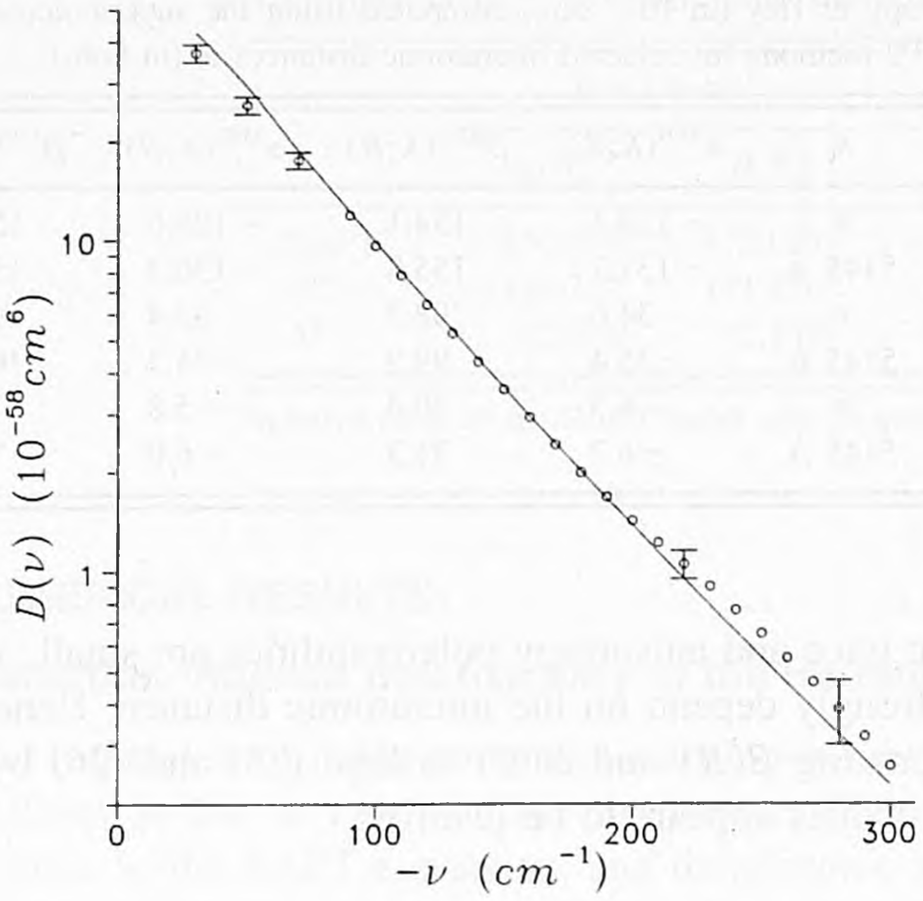

FIG. 3. Comparison of the theoretical and experimental depolarized spectra for the ^{4}He diatom. The experimental data are represented by circles.

high frequency shifts this good agreement deteriorates somewhat. Still, the predicted intensities at high frequencies are within the experimental error bars [the estimated experimental uncertainty is 6% for the frequency shifts below -150 cm^{-1}, 10% at -220 cm^{-1}, up to 35% at -300 cm^{-1} (Refs. 19 and 46)]. At very low frequencies the theoretical results are outside the experimental error bars. However, since the depolarized intensities depend on the square of the anisotropy, these discrepancies (of the order of 14%) are consistent with the estimated 5% error in our SAPT calculations, combined with the 3% error in the quantum-dynamical calculations, and the 2% error due to the neglect of the λ dependence of $\beta(R)$.

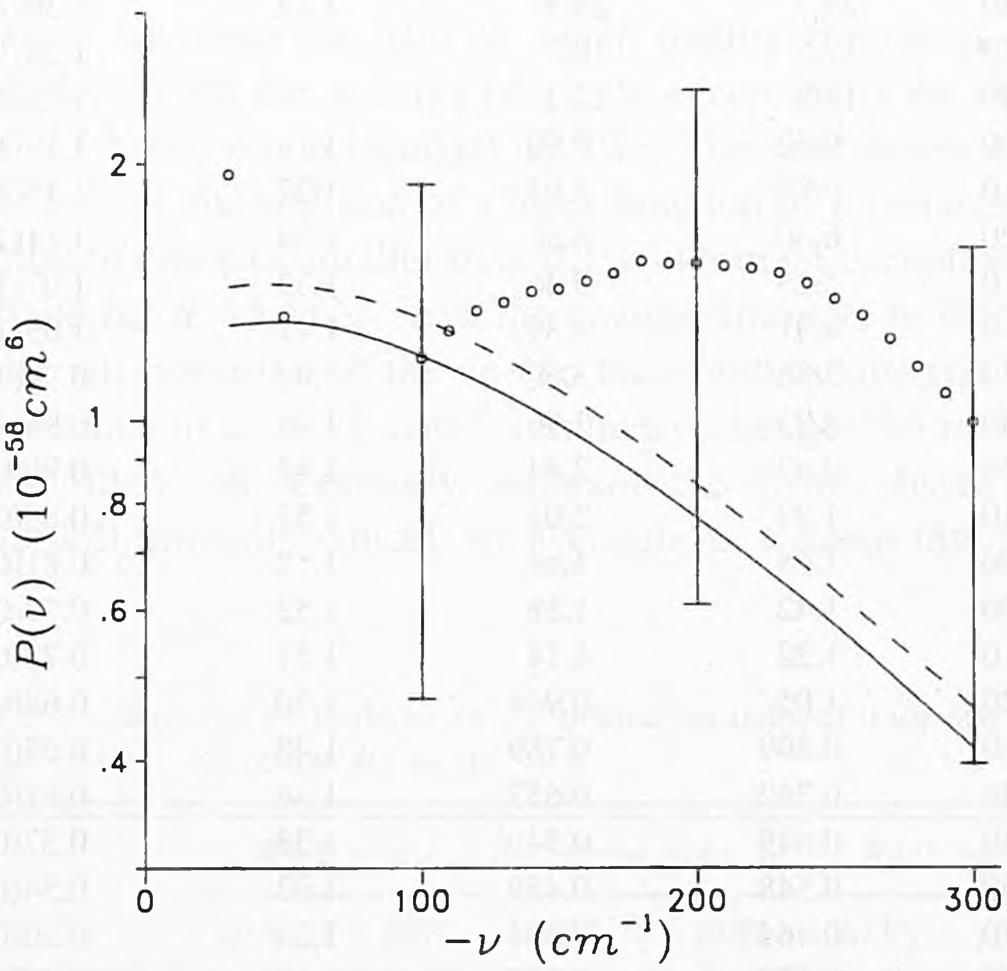

FIG. 4. Comparison of the theoretical and experimental polarized spectra for the ^{4}He diatom. The solid and dashed lines represent polarized intensities generated from the *ab initio* and scaled trace polarizabilities, respectively. The experimental data are represented by circles.

The theoretical polarized Raman intensities agree with the experiment within the large ($\pm 50\% - 60\%$) experimental error bars over a wide range of the frequency shifts. Except for the low frequency region, the predicted polarized spectrum is less intense (from 30% at $\nu = -150$ cm^{-1} to 58% at $\nu = -300$ cm^{-1}). This level of agreement between theory and experiment is not in contradiction with our estimated 5% accuracy of the interaction-induced trace polarizability, but further checks both on the theoretical and the experimental sides are visibly needed.

As discussed in the previous section, our estimate of the convergence rate of the SAPT expansion for the interaction-induced trace polarizability of He_2 is similar to the convergence rate of the perturbation series for the interaction potential.[88] The results of Ref. 88 suggest that the 5% inaccuracy in the present SAPT calculations may be partly due to the neglect of higher-order intra-atomic correlation contributions to the exchange energy. Indeed, the total exchange contribution to the He_2 interaction potential as computed from the present SAPT *ansatz* is underestimated by 2.5%. We repeated the dynamical calculations using a trace polarizability in which the exchange contribution, Eq. (16), was increased by 2.5%. The resulting polarized intensities are reported in Table VII in parentheses (see also Fig. 4). In general the agreement with the experimental results is somewhat better: This scaling increases the polarized intensities by $\sim 7\% - 10\%$, and reduces the discrepancy with the experiment from 30% to 24% at $\nu = -150$ cm^{-1}, and from 59% to 54% at -250 cm^{-1}.

The scaling of the exchange contribution to the interaction-induced trace polarizability of He_2 does not substantially improve the agreement between the theoretical and experimental polarized spectra. It is also worth noting that our results for the depolarized and polarized Raman intensities are in good agreement with those generated from Dacre's polarizability invariants.[46] Both these observations suggest that the theoretical results are rather well converged. We estimate that the error in our polarized intensities is considerably smaller than the experimental error of 50% to 60%, so that the improvement of the agreement between theory and experiment for these intensities should mainly come from the experimental side.

V. SECOND DIELECTRIC VIRIAL COEFFICIENT OF He_2

Using our *ab initio* interaction-induced trace data and the accurate empirical potential[47] we have computed the second dielectric virial coefficient over the range of temperatures in which it has been measured ($4\ K \leqslant T \leqslant 323\ K$).[20–24,26,28–30]

At high temperatures the second dielectric virial coefficient is given by the standard classical expression,[89]

$$B_{\epsilon}^{(0)}(T) = \frac{8\pi^2 N_0^2}{3} \int_0^{\infty} \alpha(R) \exp(-V(R)/k_B T) R^2 \, dR, \tag{31}$$

TABLE VIII. Comparison of the computed and measured second dielectric virial coefficients of ^{4}He (in $cm^6\ mol^{-2}$) at various temperatures (in K).

T	$B_\epsilon^{(0)}(T)$	$B_\epsilon^{(1)}(T)$	$B_\epsilon^{(2)}(T)$	$B_\epsilon(T)$	Experiment	Δ[a]	Ref.
3.799	−0.0961	0.89(+0)	−0.88(+1)	−7.9723	−0.023	?	21[b]
4.220	−0.0739	0.58(+0)	−0.49(+1)	−4.3714	0.084	±0.026	26[b]
7.199	−0.0288	0.95(−1)	−0.39(+0)	−0.3212	−0.037	±0.026	26[b]
13.804	−0.0178	0.20(−1)	−0.37(−1)	−0.0345	−0.010	±0.026	26[b]
20.271	−0.0170	0.98(−2)	−0.12(−1)	−0.0189	−0.063	±0.010	26[b]
27.098	−0.0178	0.62(−2)	−0.54(−2)	−0.0170	−0.089	±0.026	26[b]
77.4	−0.0278	0.17(−2)	−0.49(−3)	−0.0265	−0.02	±0.02	29[c]
242.95	−0.0527	0.63(−3)	−0.55(−4)	−0.0522	−0.07	±0.01	29[c]
298.15	−0.0591	0.54(−3)	−0.38(−4)	−0.0587	−0.11	±0.02	23[b]
					−0.08	±0.01	24[b]
303.0	−0.0597	0.54(−3)	−0.37(−4)	−0.0592	−0.059	±0.009	22[c]
					−0.06	±0.01	30[c]
322.15	−0.0617	0.51(−3)	−0.33(−4)	−0.0613	−0.06	±0.04	20[b]
323.0	−0.0618	0.51(−3)	−0.33(−4)	−0.0614	−0.068	±0.01	28[c]
323.15	−0.0618	0.51(−3)	−0.33(−4)	−0.0614	−0.07	±0.01	29[c]

[a]Experimental error bars.
[b]Experimental data from direct measurements.
[c]Experimental data from indirect measurements.

where N_0 is the Avogadro constant. At lower temperatures quantum corrections may become important. The semiclassical expansion of the second dielectric virial coefficient as a power series in $\hbar^2$ has been considered in Refs. 90 and 91. Ely and McQuarrie[90] derived an expression for the leading quantum correction $B_\epsilon^{(1)}(T)$, and applied it in calculations for a Lennard-Jones gas with the interaction-induced trace from the simple dipole-induced-dipole model. They concluded that at low temperatures the first quantum correction was very important and represented as much as 53%, 25%, and 13% of the classical term at $T=15.33$, 25.55, and 40.88 K, respectively. To our knowledge, approximate quantum calculations have been only reported by Fortune *et al.*[91] Unfortunately, these authors restricted their work to a single temperature, and did not compare the quantum results with the (semi)classical results.

In the present work we report a more systematic study of the importance of the quantum corrections by considering also the second-order terms, and using a realistic representation of the interaction-induced trace and the interaction potential for He_2. We approximated $B_\epsilon(T)$ as,

$$B_\epsilon(T)=B_\epsilon^{(0)}(T)+B_\epsilon^{(1)}(T)+B_\epsilon^{(2)}(T), \tag{32}$$

i.e., we computed the classical term $B_\epsilon^{(0)}(T)$, and included quantum corrections of the order $\hbar^2$ and $\hbar^4$ [denoted by $B_\epsilon^{(1)}(T)$ and $B_\epsilon^{(2)}(T)$, respectively]. The classical term $B_\epsilon^{(0)}(T)$ is given by Eq. (31), while the first quantum correction to $B_\epsilon^{(0)}(T)$ can be written as,

$$B_\epsilon^{(1)}(T)=-\frac{\pi^2\hbar^2N_0^2}{9\mu k_B^2T^2}\int \exp(-V(R)/k_BT) \times\left[\frac{\alpha(R)}{k_BT}\left(\frac{dV}{dR}\right)^2-2\frac{dV}{dR}\frac{d\alpha}{dR}\right]R^2\,dR. \tag{33}$$

To our knowledge the explicit formula for the second quantum correction to the dielectric virial coefficient has not been reported in the literature thus far. The derivation is based on the relation between the pressure virial coefficient of the gas in a uniform static electric field and the dielectric virial coefficient.[92,93] The resulting expression for $B_\epsilon^{(2)}(T)$ is somewhat more involved, and can be written as,

$$B_\epsilon^{(2)}(T)=\frac{\pi^2\hbar^4N_0^2}{180\mu^2k_B^3T^3}\int \exp(-V(R)/k_BT) \times\left[\frac{\alpha(R)}{k_BT}f(R)+g(R)\right]R^2\,dR, \tag{34}$$

where the functions $f(R)$ and $g(R)$ are given by

$$f(R)=\left(\frac{d^2V}{dR^2}\right)^2+\frac{2}{R^2}\left(\frac{dV}{dR}\right)^2+\frac{10}{9k_BT}\frac{1}{R}\left(\frac{dV}{dR}\right)^3-\frac{5}{36k_B^2T^2}\left(\frac{dV}{dR}\right)^4, \tag{35}$$

$$g(R)=-2\frac{d^2V}{dR^2}\frac{d^2\alpha}{dR^2}-\frac{4}{R^2}\frac{dV}{dR}\frac{d\alpha}{dR}-\frac{10}{3k_BT}\frac{1}{R}\left(\frac{dV}{dR}\right)^2\frac{d\alpha}{dR}+\frac{5}{9k_B^2T^2}\left(\frac{dV}{dR}\right)^3\frac{d\alpha}{dR}. \tag{36}$$

The integration over R has been done in the range from $R=3$ bohr to $R=100$ bohr using a composite Simpson rule. In the inner region ($R<3$ bohr) the function $\exp(-V/kT)$ is effectively zero, while in the outer region, $R>100$ bohr, all contributions are negligibly small. The number of radial points was $N=2^{n-1}+1$. We increased n by 1 in each iteration and stopped when the relative error was smaller than 10^{-6}. We checked that our results are stable against changes in the boundaries and/or integration parameters.

The results of our calculations, presented in Table VIII and Fig. 5, are compared with the available experimental data.[20–24,26,28–30] Also presented in this table is the classical

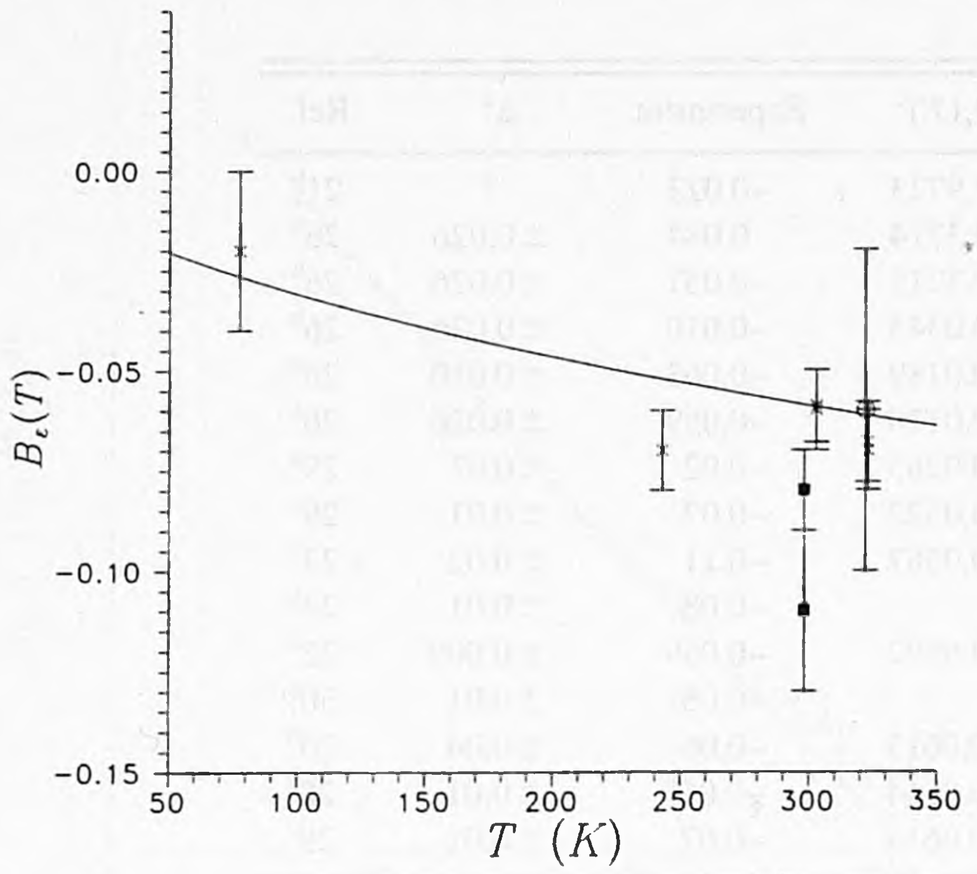

FIG. 5. Comparison of the *ab initio* and experimental second dielectric virial coefficients of ^{4}He at various temperatures. The solid line represents the second dielectric virial coefficients generated from the *ab initio* SAPT polarizability trace, and the empirical potential of Ref. 47. Crosses label the indirect measurements from Refs. 22, 28–30, open circles the measurements from Ref. 20, and filled squares represent experimental data from Refs. 23 and 24.

dielectric virial coefficient computed with the aid of Eq. (31), and the first, and second quantum corrections. An inspection of Table VIII shows that the quantum effects are very small for temperatures larger than 70 K, and $B_\epsilon(T)$ can be efficiently computed from the classical expression. At lower temperatures the dielectric virial coefficient of the ^{4}He gas starts to deviate from the classical value, and at very low temperatures the semiclassical expansion of the second dielectric virial coefficient in powers of $\hbar^2$ clearly diverges.

At high temperatures our results agree well with the data from indirect measurements.[22,28–30] The only exception is the value at $T=242.95$ K. Here the theoretical result is slightly outside the experimental error bars. The agreement with the results of direct measurements[20,23,24] is less satisfactory. The present *ab initio* results agree very well with the old experimental data of Orcutt and Cole,[20] and disagree with the data of Vidal and Lallemand.[23,24] Since our results agree with the majority of the high-temperature experimental data, and since the second dielectric virial coefficient changes very slowly with temperature, it is very likely that the results of direct measurements reported by Vidal and Lallemand[24] are contaminated by nonadditive three-body effects.

At low temperatures the situation is more complex. Our result at 77.4 K agrees very well with the value from indirect measurements reported by Huot and Bose.[29] Other low temperature experimental data[21,26] cannot be compared with our theoretical values due to the divergence of the semiclassical expansion, and full quantum calculations are needed. Work in this direction is in progress.[93]

VI. SUMMARY AND CONCLUSIONS

Symmetry-adapted perturbation theory has been applied to compute the invariants of the interaction-induced polarizability for the He diatom. The accuracy of the computed response properties has been checked by comparison with benchmark full CI results, and by extensive studies of the basis set convergence. We have estimated that the present SAPT results for the interaction-induced trace and anisotropy of He_2 should be accurate to about 5%.

Using the computed trace and anisotropy we have performed converged quantum-dynamical calculations of the depolarized and polarized binary Raman spectra. The predicted depolarized intensities are in good agreement with the experimental data[19] over a wide range of the frequency shifts. The agreement between theory and experiment for the polarized spectrum is within the experimental error bars, although the theoretical spectrum is less intense than the experimental one. The analysis of the accuracy of the present calculations suggests that the error in the predicted polarized intensities is much smaller than the experimental error bars, so the improvement of agreement between theory and experiment must mainly come from the experimental side.

Further checks of the accuracy of the computed trace polarizability have been performed by computing the second dielectric virial coefficients (including first and second quantum corrections) at various temperatures and by comparing with the available experimental data.[20–24,26,28–30] Our results agree well with the majority of the high-temperature experimental data. The low temperature experimental results of Kerr and Sherman,[21] and Gugan and Michel[26] could not be used to assess the accuracy of the computed trace polarizability due to the divergence of the semiclassical expansion.

ACKNOWLEDGMENTS

We would like to thank Professor R. J. Le Roy for sending us his BCONT program, and Professor L. Frommhold for providing us with his Raman data for He_2. We also thank Professor L. Frommhold for reading and commenting on the manuscript. This work was supported by the Netherlands Foundation of Chemical Research (SON), the Netherlands Organization for Scientific Research (NWO), and Polish Scientific Research Council (KBN), Grant No. 3 T09A 072 09.

[1] *Phenomena Induced by Intermolecular Interactions*, edited by G. Birnbaum, NATO ASI Series B, Vol. 127 (Plenum, New York, 1985).
[2] *Collision- and Interaction-Induced Spectroscopy*, edited by G. C. Tabisz and M. N. Neuman, NATO ASI Series C, Vol. 452 (Kluwer, Dordrecht, 1995).
[3] H. B. Levine and G. Birnbaum, Phys. Rev. Lett. **20**, 439 (1968).
[4] J. P. McTague and G. Birnbaum, Phys. Rev. Lett. **21**, 661 (1968).
[5] J. P. McTague and G. Birnbaum, Phys. Rev. A **3**, 1376 (1971).
[6] L. Frommhold, Adv. Chem. Phys. **46**, 1 (1981).
[7] A. Borysow and L. Frommhold, Adv. Chem. Phys. **75**, 439 (1989).
[8] L. Ulivi and L. Frommhold (unpublished).
[9] T. K. Bose, in *Phenomena Induced by Intermolecular Interactions*, edited by G. Birnbaum, NATO ASI Series B, Vol. 127 (Plenum, New York, 1985), p. 49.
[10] T. K. Bose, in *Collision- and Interaction-Induced Spectroscopy*, edited by G. C. Tabisz and M. N. Neuman, NATO ASI Series C, Vol. 452 (Kluwer, Dordrecht, 1995), p. 77.
[11] E. R. Pike and J. M. Vaughan, J. Phys. C **4**, L362 (1971).
[12] Y. Le Duff, Phys. Rev. A **20**, 48 (1979).
[13] F. Barocchi, P. Mazzinghi, and M. Zoppi, Phys. Rev. Lett. **41**, 1785 (1978).
[14] F. Barocchi, P. Mazzinghi, and M. Zoppi, in *Intermolecular Spectroscopy*

and Dynamical Properties of Dense Systems, Proceedings of the International School "Enrico Fermi", Course LXXV, edited by J. van Kranendonk (North-Holland, Amsterdam, 1981), p. 263.
[15] M. Proffitt and L. Frommhold, Phys. Rev. Lett. **42**, 1473 (1979).
[16] L. Frommhold and M. Proffitt, J. Chem. Phys. **70**, 4803 (1979).
[17] M. Proffitt and L. Frommhold, J. Chem. Phys. **72**, 1377 (1980).
[18] M. Proffitt, J. W. Keto, and L. Frommhold, Phys. Rev. Lett. **45**, 1843 (1980).
[19] M. Proffitt, J. W. Keto, and L. Frommhold, Can. J. Phys. **59**, 1459 (1981).
[20] R. H. Orcutt and R. H. Cole, J. Chem. Phys. **46**, 697 (1967).
[21] E. C. Kerr and R. H. Sherman, J. Low Temp. Phys. **3**, 451 (1970).
[22] S. Kirouac and T. K. Bose, J. Chem. Phys. **64**, 1580 (1976).
[23] D. Vidal and M. Lallemand, J. Chem. Phys. **64**, 4293 (1976).
[24] M. Lallemand and D. Vidal, J. Chem. Phys. **66**, 4776 (1977).
[25] B. J. Alder, J. C. Beers II, H. L. Strauss, and J. J. Weis, Proc. Nat. Acad. Sci. USA **77**, 3098 (1980).
[26] D. Gugan and G. W. Michel, Metrologia **16**, 149 (1980).
[27] D. Gugan, Metrologia **19**, 147 (1962).
[28] H. J. Achtermann, G. Magnus, and T. K. Bose, J. Chem. Phys. **94**, 5669 (1991).
[29] J. Huot and T. K. Bose, J. Chem. Phys. **95**, 2683 (1991).
[30] H. J. Achtermann, J. G. Hong, G. Magnus, R. A. Aziz, and J. Slaman, J. Chem. Phys. **98**, 2308 (1993).
[31] Y. Le Duff, J. Phys. Lettres **40**, 267 (1979).
[32] R. A. Harris, D. F. Heller, and W. M. Gelbart, J. Chem. Phys. **61**, 3854 (1974).
[33] E. F. O'Brien, V. P. Gutschick, V. McKoy, and J. P. McTague, Phys. Rev. A 8, 690 (1973).
[34] P. J. Fortune and P. R. Certain, J. Chem. Phys. **61**, 2620 (1974).
[35] G. P. Arrighini, C. Guidotti, and U. T. Lamanna, Chem. Phys. **16**, 29 (1976).
[36] J. W. Kress and J. J. Kozak, J. Chem. Phys. **66**, 4516 (1977).
[37] M. G. Papadopoulos and J. Waite, Chem. Phys. Lett. **135**, 361 (1987); J. Waite and M. G. Papadopoulos, Theor. Chim. Acta **75**, 53 (1989).
[38] P. D. Dacre, Mol. Phys. **36**, 541 (1978).
[39] P. D. Dacre, Mol. Phys. **45**, 17 (1982).
[40] P. R. Certain and P. J. Fortune, J. Chem. Phys. **55**, 5818 (1971).
[41] D. M. Bishop and J. Pipin, J. Chem. Phys. **97**, 3375 (1992); **99**, 4875 (1993).
[42] P. W. Fowler, K. L. C. Hunt, H. M. Kelly, and A. J. Sadlej, J. Chem. Phys. **100**, 2932 (1994).
[43] A. T. Prengel and W. S. Gornall, Phys. Rev. A **13**, 253 (1976).
[44] L. Frommhold, K. Hong Hong, and M. H. Proffitt, Mol. Phys. **35**, 665 (1978).
[45] J. Borysow and L. Frommhold, in *Phenomena Induced by Intermolecular Interactions*, edited by G. Birnbaum, NATO ASI Series B, Vol. 127 (Plenum, New York, 1985), p. 67.
[46] P. D. Dacre and L. Frommhold, J. Chem. Phys. **76**, 3447 (1982).
[47] R. A. Aziz, F. R. McCourt, and C. C. K. Wong, Mol. Phys. **61**, 1487 (1987).
[48] R. A. Aziz and M. J. Slaman, J. Chem. Phys. **94**, 8047 (1991).
[49] T. G. A. Heijmen, R. Moszynski, P. E. S. Wormer, and A. van der Avoird, Mol. Phys. (in press).
[50] K. Szalewicz and B. Jeziorski, Mol. Phys. **38**, 191 (1979).
[51] B. Jeziorski, R. Moszynski, S. Rybak, and K. Szalewicz, in *Many-Body Methods in Quantum Chemistry*, Lecture Notes in Chemistry, edited by U. Kaldor (Springer, New York, 1989), Vol. 52, p. 65.
[52] S. Rybak, B. Jeziorski, and K. Szalewicz, J. Chem. Phys. **95**, 6576 (1991).
[53] R. Moszynski, B. Jeziorski, A. Ratkiewicz, and S. Rybak, J. Chem. Phys. **99**, 8856 (1993).
[54] R. Moszynski, B. Jeziorski, and K. Szalewicz, J. Chem. Phys. **100**, 1312 (1994).
[55] R. Moszynski, B. Jeziorski, S. Rybak, K. Szalewicz, and H. L. Williams, J. Chem. Phys. **100**, 5080 (1994).
[56] R. Moszynski, S. M. Cybulski, and G. Chalasinski, J. Chem. Phys. **100**, 4998 (1994).
[57] B. Jeziorski and W. Kolos, Int. J. Quantum Chem. (Suppl. 1) **12**, 91 (1977).
[58] B. Jeziorski and W. Kolos, in *Molecular Interactions*, edited by H. Ratajczak and W. J. Orville-Thomas (Wiley, New York, 1982), Vol. 3, p. 1.
[59] T. Cwiok, B. Jeziorski, W. Kolos, R. Moszynski, and K. Szalewicz, J. Chem. Phys. **97**, 7555 (1992).
[60] T. Cwiok, B. Jeziorski, W. Kolos, R. Moszynski, and K. Szalewicz, J. Mol. Struct. (Theochem) **307**, 135 (1994).
[61] B. Jeziorski, R. Moszynski, and K. Szalewicz, Chem. Rev. **94**, 1887 (1994).
[62] R. Moszynski, B. Jeziorski, G. H. F. Diercksen, and L. A. Viehland, J. Chem. Phys. **101**, 4697 (1994).
[63] R. Moszynski, P. E. S. Wormer, and L. A. Viehland, J. Phys. B **27**, 4933 (1994).
[64] H. L. Williams, K. Szalewicz, B. Jeziorski, R. Moszynski, and S. Rybak, J. Chem. Phys. **98**, 1279 (1993).
[65] R. Moszynski, P. E. S. Wormer, B. Jeziorski, and A. van der Avoird, J. Chem. Phys. **101**, 2811 (1994).
[66] R. Moszynski, P. E. S. Wormer, and A. van der Avoird, J. Chem. Phys. **102**, 8385 (1995).
[67] R. Moszynski, T. Korona, P. E. S. Wormer, and A. van der Avoird, J. Chem. Phys. **103**, 321 (1995).
[68] M. Jeziorska, B. Jeziorski, and J. Cizek, Int. J. Quantum Chem. **32**, 149 (1987).
[69] R. Moszynski, T. G. A. Heijmen, and B. Jeziorski, Mol. Phys. (in press).
[70] A. J. Sadlej, Mol. Phys. **39**, 1249 (1980).
[71] M. Jaszunski, Mol. Phys. **39**, 777 (1980).
[72] B. Jeziorski, M. Bulski, and L. Piela, Int. J. Quantum Chem. **10**, 281 (1976).
[73] G. Chalasinski and B. Jeziorski, Theor. Chim. Acta **46**, 277 (1977).
[74] F. B. van Duijneveldt, IBM Research Report, RJ945 (1971); the exponents and contraction coefficients of the *s* functions for the He atom are available from the present authors on request.
[75] M. Gutowski, J. Verbeek, J. H. van Lenthe, and G. Chalasinski, Chem. Phys. **111**, 396 (1987).
[76] B. Jeziorski, R. Moszynski, A. Ratkiewicz, S. Rybak, K. Szalewicz, and H. L. Williams, in *Methods and Techniques in Computational Chemistry: METECC-94, vol. B Medium Size Systems*, edited by E. Clementi (STEF, Cagliari, 1993), p. 79.
[77] S. Zarrabian, C. R. Sarma, and J. Paldus, Chem. Phys. Lett. **155**, 183 (1989); R. J. Harrison and S. Zarrabian, *ibid.* **158**, 393 (1989).
[78] P. E. S. Wormer and H. Hettema, J. Chem. Phys. **97**, 5592 (1992).
[79] P. E. S. Wormer and H. Hettema, POLCOR package (Nijmegen 1992).
[80] S. F. Boys and F. Bernardi, Mol. Phys. **19**, 553 (1970).
[81] K. T. Tang and J. P. Toennies, J. Chem. Phys. **80**, 3726 (1984).
[82] A. Weber, in *The Raman Effect*, edited by A. Anderson (M. Dekker, New York, 1973), Vol. 2, p. 543.
[83] P. E. S. Wormer, E. H. T. Olthof, R. A. H. Engeln, and J. Reuss, Chem. Phys. **178**, 189 (1993).
[84] D. M. Brink and G. R. Satchler, *Angular Momentum* (Clarendon, Oxford, 1975).
[85] R. J. Le Roy, Comput. Phys. Comm. **52**, 383 (1989).
[86] R. J. Le Roy, University of Waterloo Chemical Physics Research Report CP-329R (1993).
[87] *Handbook of Chemistry and Physics*, edited by R. C. Weast and M. J. Asth (Chemical Rubber, Boca Raton, 1981).
[88] T. Korona *et al.* (unpublished).
[89] A. D. Buckingham and J. A. Pople, Trans. Faraday Soc. **51**, 1029, 1079 (1955).
[90] J. F. Ely and D. A. McQuarrie, J. Chem. Phys. **54**, 2885 (1971).
[91] L. W. Bruch, P. J. Fortune, and D. H. Berman, J. Chem. Phys. **61**, 2626 (1974).
[92] T. L. Hill, J. Chem. Phys. **28**, 61 (1958).
[93] R. Moszynski, T. G. A. Heijmen, and A. van der Avoird, Chem. Phys. Lett. **247**, 440 (1995).